I. Introduction

Upcoming formation flying space missions like eLISA (evolved Laser Interferometer Space Antenna)[1] or NGGM (Next Generation Gravity Mission)[2] create a new demand for highly precise attitude control. The demands lie in the micronewton regime for thrust and noise levels with continued operation for several years. One promising candidate to reach these goals is the High Efficiency Multistage Plasma Thruster (HEMPT). An effort to downscale this thruster into this thrust and noise regime is undertaken in cooperation of Airbus Defence and Space, the Center of Applied Space Technology and Microgravity (ZARM) of the University Bremen and the German Aerospace Center (DLR). This campaign consists of a breadboard level model of the thruster,[3] a highly precise thrust balance,[4] and computer modeling to support the development.[5] We present results of one of the first simulations of a downscaled HEMPT, including its discharge chamber and its near exit region.

II. Model setup

The HEMPT uses a direct current discharge for ion generation, where electron confinement is improved by a static magnetic field with a cusped topology.[6] Fig. 2 shows a schematic of this thruster type. The domain for the simulation of the downscaled thruster investigated here is an $r - z$ plane which corresponds to a cylinder with the radius $R = 5.12$ mm and the length $Z = 20.48$ mm. It includes not only the thruster's discharge chamber, but also its near exit region. The static magnetic field within this domain is imported from a finite element simulation using the software FEMM, based on the geometric and material properties of the permanent magnet arrangement. The result of a particle based simulation of the neutral gas for an inflow of 0.27 sccm xenon is imported to create the neutral gas distribution inside the simulation domain. The neutral particles continue their motion while new ones are inserted with the same mass flow over the course of the plasma simulation.

The plasma is simulated using the particle-in-cell method,[7] the calculation is performed by the Vorpal engine.[8] It applies a number ratio of the so-called super particles to the real particles of $1 : 1.6 \cdot 10^3$ for the xenon ions and electrons. With respect to their much higher density, for the neutrals the ratio is $1 : 6 \cdot 10^5$. Accurate reduction of the neutrals is nevertheless achieved, due to the use of variable weight particles.[9] Elastic, excitation and ionization collisions are treated by a Monte Carlo algorithm.[10] For the collisions, the energy dependent collision cross-sections are taken from Ref.[11] Long range electrostatic interactions are resolved on the simulation grid, which has 1024 times 256 cells. The volume 0 mm $\leq z \leq$ 14 mm, 2.5 mm $\leq r \leq 5.12$ mm is grounded, in order to represent the magnets and their distance rings. All domain boundaries are grounded as well, with the exception of the symmetry axis (z-axis) and the anode, which lies at $z = 0$ mm in the range from 0 mm $\leq r \leq$ 1.5 mm on a potential of 400 V. At $r = 1.5$ mm over the distance 0 mm $\leq z \leq$ 14 mm, surface charge accumulation on the ceramic tube, that forms the discharge chamber, is taken into account. An equal surface is at $z = 14$ mm, 1.5 mm $\leq r \leq$ 2.5 mm, which forms the top end of the ceramic tube. All other boundaries for the charged particles are the electrostatic ones and are simply absorbing. For the neutral particles, the anode and ceramic surfaces are diffusively reflective. The electron
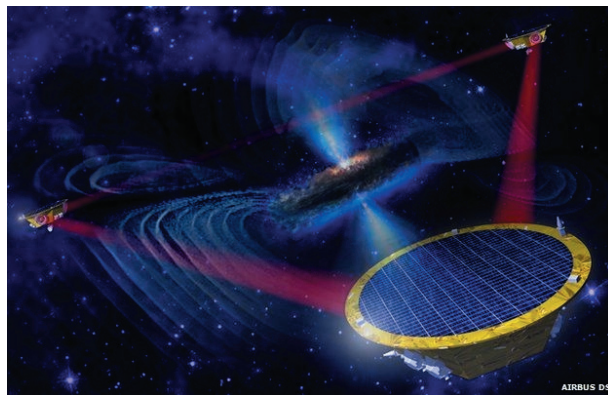

Figure 1. The future Laser Interferometer Space Antenna (LISA) for the detection of gravitational waves.
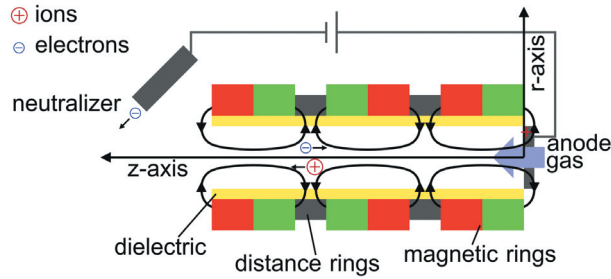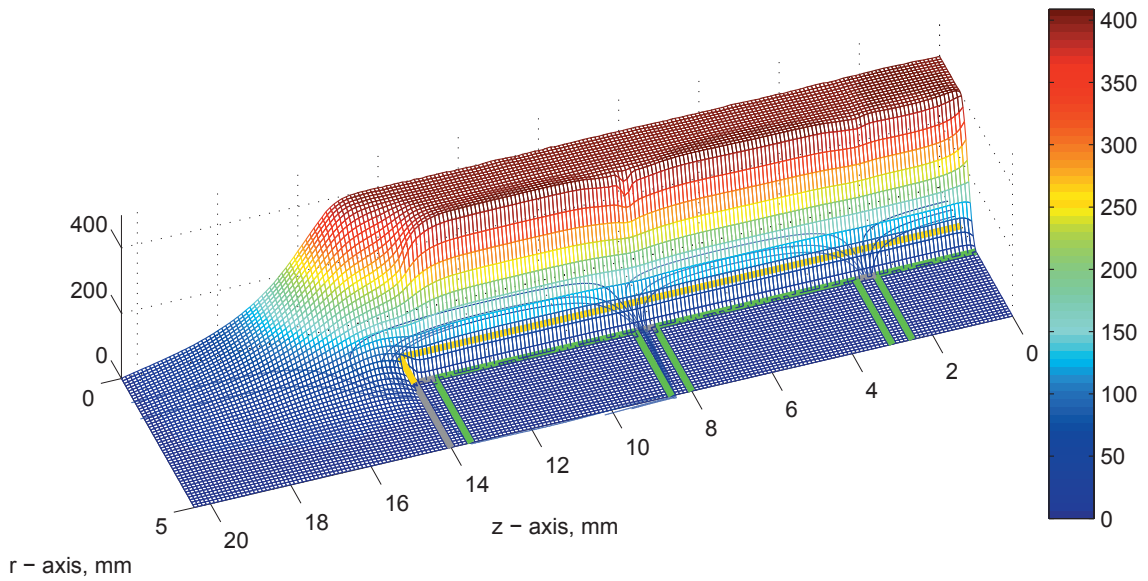
Figure 2. HEMP thruster principle.

Figure 3. Electric potential in V. Dielectric surface (yellow), distance rings (gray), magnets (green), magnetic field lines (blue).

source lies in the simulated thruster's exit region, at 18.0 mm $\leq z \leq$ 18.3 mm, 0 mm $\leq r \leq$ 4.5 mm. Particle positions are defined in r and z coordinates, but all three velocity vector components v_r, v_z, and v_φ are calculated in order to represent the electron gyration motion in the magnetic field.

To reduce the time needed by the computational process to get a stable result, the size of the system is scaled down by a factor of 10. In order to preserve the relation of both the charged particles mean free paths and their gyration radii to the system length, the electron source strength and neutral gas inflow is reduced by the same factor, while the magnetic field strength is increased by this factor.[12] The cell size is $2 \cdot 10^{-6}$ mm in both directions, in order to resolve the smallest Debye length resulting from the plasma density ($1 \cdot 10^{18}$ - $1 \cdot 10^{19}$ m^{-3}) and temperature (1 - 10 eV) expected for this type of thruster. The time step size was set to $2 \cdot 10^{-13}$ s in order to resolve the electron gyration motion at the strongest magnetic field strength. The simulation was run over $3.7 \cdot 10^5$ time steps.

III. Results

One of the plasma parameters that cannot be measured directly due to the small size of the device is the electric potential. Fig. 3 shows the profile of this potential after an evolution of the plasma discharge at a simulated time of $7.4 \cdot 10^{-8}$ s (smoothed over each 5 times 5 cells). The potential is mostly flat throughout
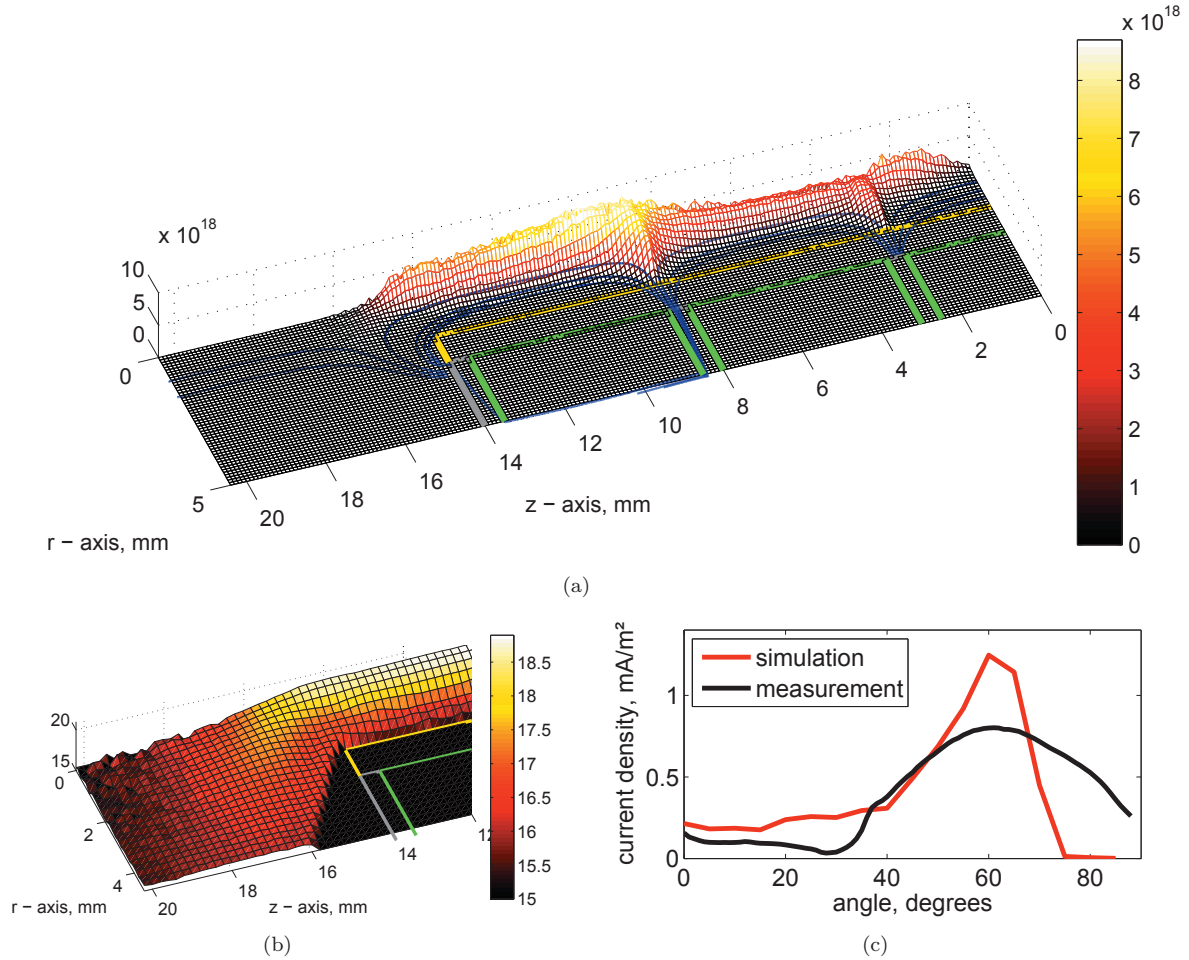
(a)

(b)

(c)

Figure 4. Ion density in $1/m^3$ for (a) the entire domain and (b) the near exit region (logarithmic). (c) angular ion beam current distribution. Dielectric surface (yellow), distance rings (gray), magnets (green), magnetic field lines (blue).

the discharge channel, with a value close to the anode potential. Retarding potential analyzer measurements for the downscaled HEMPT that is modeled here also suggest a single, major potential drop for most of the ions.[13] While most of the discharge channel wall has charged up to nearly anode potential, small exceptions are at the positions of the magnetic cusps. Where the magnetic field is perpendicular to the wall, most of the electrons reach the wall and create a negative surface charge. The main potential drop near the thruster's exit is roughly of diagonal shape. This consequently accelerates the ions obliquely away from the symmetry axis, showing the reason for the hollow cone shaped plume which is typical for HEMP thrusters.

The ion density of the entire simulation domain is presented in Fig. 4 (a) (smoothed over each 5 times 5 cells). It illustrates, that the ion profile is influenced by the shape of the magnetic field. Since the ions are too heavy to be influenced directly by the given magnetic field strength at the system size, the influence can only be mediated through the electrons. The mobility of the electrons perpendicular to the magnetic field lines is strongly reduced. In Fig. 4 (b), the ion density profile is presented in the logarithmic scale so that the plume region with its lower density is clearly visible.

A more detailed analyses, however, is needed to investigate the ion current's angular dependency. Therefore, 36 virtual measurement points are placed at the radial and axial boundaries of the near exit region. They can determine the ion flux in 5 degree steps where the angle is defined by the line from the measurement point to the midpoint of the ion beam's origin and the symmetry axis of the thruster. There is inevitably

some small systematic error because the radial size of the discharge chamber exit is not negligible. The simulated values can now be compared to Faraday cup measurements at the real thruster. The Faraday cup is on a 40 cm long beam turned around the discharge chamber exit in one degree steps. Fig. 4 (c) shows the results for both measurements and simulations, calculated for 1 m distance. The peak of the simulated ion current is about one and a half time higher, while the angular profile shows some similarity with the measurements. In both cases the maxima lies about 60 degrees. In the simulation the electron current at the anode is 3.8 mA, the measured value is 4.5 mA.

IV.   Conclusions and Outlook

The simulation of this downscaled HEMP thruster shows a flat potential inside the thruster, which is typical for normal sized HEMPTs. The ion density profile is structured. The angular distribution of the ion beam in the simulation reproduces the hollow cone seen in the experiment, with some deviations. Upcoming simulations will include additional effects such as secondary electron emission, Bohm diffusion, and double ionization. Such extensions will make the model more realistic, and should bring its results closer to reality. This in turn should give more insight in this particular thruster type and will provide possibilities for performance improvements.

Acknowledgments

References

[1] Pau Amaro-Seoane et al. Class. Quantum Grav. 29, 124016 (2012).

[2] P. Silvestrin, M. Aguirre, L. Massotti, S. Cesare. Next Generation Gravity Mission: a Step Forward in the Earth's Gravity Field Determination.

[3] A. Keller, P. Köhler, F. G. Hey, M. Berger, C. Braxmaier, D. Feili, D. Weise, U. Johann. Parametric Study of HEMP-Thruster, Downscaling to μN Thrust Levels. *In proceeding of: 33rd International Electric Propulsion Conference, At The George Washington University, Washington, D.C., USA.*

[4] F. G. Hey, A. Keller, D. Papendorf, C. Braxmaier, M. Tajmar, U. Johann, D. Weise. Development of a Highly Precise Micro-Newton Thrust Balance. *In proceeding of: 33rd International Electric Propulsion Conference, At The George Washington University, Washington, D.C., USA.*

[5] T. Brandt, T. Trottenberg, R. Groll, F. Jansen, F. G. Hey, U. Johann, H. Kersten, C. Braxmaier. Particle-in-Cell simulation of the plasma properties and ion acceleration of a down-scaled HEMP-Thruster. *4th International Spacecraft Propulsion Conference, May 19th - 22th, 2014, Cologne, Germany.*

[6] K. N. Leung, N. Hershkowitz, K. R. MacKenzie. Plasma confinement by localized cusps. *Physics of Fluids (1958-1988) 19, 1045 (1976); doi: 10.1063/1.861575.*

[7] R.W. Hockney, J.W. Eastwood. Computer Simulation Using Particles. *Adam Hilger, 1988.*

[8] C. Nieter, J. R. Cary. VORPAL: a versatile plasma simulation code. *Journal of Computational Physics 196 (2004) 448473.*

[9] Hutchinson, D. A. W.; Turner, M. M. Variable statistical weights for particle species in pic-mcc simulations. *AIP Conference Proceedings, Volume 380, pp. 26-35 (1996).*

[10] J.Spanier, E.M.Gelbard. Monte Carlo Principles and Neutron Transport Problems. *Addison Wesley 1969.*

[11] S. T. Perkins, D. E. Cullen, S. M. Seltzer. Tables and graphs of electron-interaction cross sections from 10 eV to 100 GeV derived from the LLNL Evaluated Electron Data Library (EEDL), Z = 1 to 100. *November 12, 1991.*

[12] Francesco Taccogna, Savino Longo, Mario Capitelli, Ralf Schneider Self-similarity in Hall plasma discharges: Applications to particle models. Francesco Taccogna, Savino Longo, Mario Capitelli, Ralf Schneider.

[13] A. Keller, P. Köhler, D. Feili, M. Berger, C. Braxmaier, D. Weise, U. Johann. Feasibility of a down-scaled HEMP-Thruster. *IEPC-2011-138.*